Discovery of *N*-(4-(2-Amino-3-chloropyridin-4-yloxy)-3-fluorophenyl)-4-ethoxy-1-(4-fluorophenyl)-2-oxo-1,2-dihydropyridine-3-carboxamide (BMS-777607), a Selective and Orally Efficacious Inhibitor of the Met Kinase Superfamily

Gretchen M. Schroeder,* Yongmi An, Zhen-Wei Cai, Xiao-Tao Chen, Cheryl Clark, Lyndon A. M. Cornelius, Jun Dai, Johnni Gullo-Brown, Ashok Gupta, Benjamin Henley, John T. Hunt, Robert Jeyaseelan, Amrita Kamath, Kyoung Kim, Jonathan Lippy, Louis J. Lombardo, Veeraswamy Manne, Simone Oppenheimer, John S. Sack, Robert J. Schmidt, Guoxiang Shen, Kevin Stefanski, John S. Tokarski, George L. Trainor, Barri S. Wautlet, Donna Wei, David K. Williams, Yingru Zhang, Yueping Zhang, Joseph Fargnoli, and Robert M. Borzilleri

Bristol-Myers Squibb Research and Development, P.O. Box 4000, Princeton, New Jersey, 08543-4000

Abstract: Substituted *N*-(4-(2-aminopyridin-4-yloxy)-3-fluoro-phenyl)-1-(4-fluorophenyl)-2-oxo-1,2-dihydropyridine-3-carboxamides were identified as potent and selective Met kinase inhibitors. Substitution of the pyridine 3-position gave improved enzyme potency, while substitution of the pyridone 4-position led to improved aqueous solubility and kinase selectivity. Analogue **10** demonstrated complete tumor stasis in a Met-dependent GTL-16 human gastric carcinoma xenograft model following oral administration. Because of its excellent in vivo efficacy and favorable pharmacokinetic and preclinical safety profiles, **10** has been advanced into phase I clinical trials.

Met kinase, also known as hepatocyte growth factor receptor, is an oncogenic transmembrane receptor tyrosine kinase that has been implicated in a variety cancers.[1,2] Binding of its endogenous ligand hepatocyte growth factor (HGF), also known as scatter factor (SF), results in dimerization of the Met kinase receptor and intermolecular transphosphorylation of multiple tyrosine residues in the intracellular domain. The resulting activated enzyme binds and phosphorylates adaptor proteins at a multifunctional docking site, which in turn activates signal transducers to mediate a variety of cellular responses including cell growth, migration and invasion, tumor metastasis, angiogenesis, wound healing, and tissue regeneration. While normal Met/HGF signaling plays a critical role in placental development and liver regeneration,[3] aberrant Met signaling can lead to oncogenic transformation. Met kinase can become dysregulated via a variety of mechanisms including ligand-dependent activation, activating mutations, Met overexpression, and interactions with other receptor families (heterodimerization/cross-talk).[1]

The structure−activity relationships (SARs) of several Met kinase inhibitors derived from pyrrolo[2,1-*f*][1,2,4]triazine,[4] pyrrolopyridine,[5] and aminopyridine[5] scaffolds were recently

* To whom correspondence should be addressed. Phone: 609-252-3965. Fax: 609-252-7410. E-mail: gretchen.schroeder@bms.com.

disclosed. Replacement of the pendent acylurea moiety by a conformationally constrained 2-pyridone to give Met kinase inhibitors with potent antiproliferative activity in a Met-dependent human gastric carcinoma GTL-16 cell line was subsequently reported.[6] Herein, we describe application of the 2-pyridone fragment to the aminopyridine chemotype, which ultimately led to identification of a compound for clinical development. The synthesis, SAR, structural biology, and preclinical assessment of aminopyridines are described.
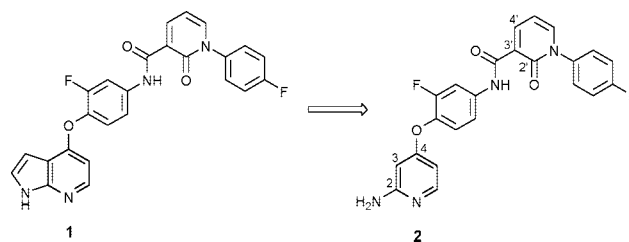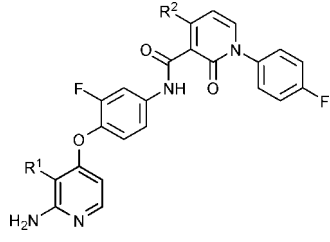

Pyridone **1**[6] is a potent inhibitor of Met kinase (IC$_{50}$ = 1.8 nM) with excellent activity in the Met-driven GTL-16 cell proliferation assay (IC$_{50}$ = 60 nM). Application of the conformationally constrained 2-pyridone ring to the aminopyridine series gave parent pyridone **2** (IC$_{50}$ = 4.5 nM, GTL-16 IC$_{50}$ = 170 nM), which served as a starting point for SAR analysis. On the basis of X-ray crystal structures of related analogues,[4−6] we hypothesized that these inhibitors would occupy the Met ATP-binding site and that substitution of the pyridine C-3 position would provide access to the pocket occupied by the ribose group of ATP. As described in an earlier series, additional interactions with the Met protein could be gained by projecting solubilizing groups such as alcohols and amines into the ribose pocket.[4] We initially sought to introduce such groups in the aminopyridine series via a linker at the pyridine C-3 position to simultaneously improve potency, solubility, and the CYP450 inhibition profile.

Alcohols and amines were appended to the aminopyridine core via a carbon linker, and representative analogues are depicted in Table 1. *N*-Methylpiperazine **3** gave excellent potency in the biochemical assay (IC$_{50}$ = 5.9 nM), demonstrating that substitution at the pyridine C-3 position was tolerated. However, disappointing results were obtained in the GTL-16 cell-based assay (GTL-16 IC$_{50}$ = 2800 nM). In our previous work, rigid amines with limited degrees of freedom gave enhanced Met potency. Application of this concept as in propargylamine **4** gave similar biochemical potency but improved cellular activity (IC$_{50}$ = 3.8 nM, GTL-16 IC$_{50}$ = 210 nM). The corresponding propargyl alcohol **5** gave an exceptionally potent Met inhibitor in the biochemical and cell-based assays (IC$_{50}$ = 2.7 nM, GTL-16 IC$_{50}$ = 23 nM). Methanol adduct **6** gave similar biochemical inhibition (IC$_{50}$ = 3.4 nM) but was 10-fold less potent in cells relative to the propargyl alcohol (GTL-16 IC$_{50}$ = 280 nM).

Intrigued by the excellent cellular potency of propargylic alcohol **5** and with the desire to keep the pyridine C-3 substituent small, we prepared the unsubstituted propargylic compound **7**. This analogue also demonstrated potent inhibition of Met kinase in biochemical and cell-based assays (IC$_{50}$ = 1.0 nM, GTL-16 IC$_{50}$ = 31 nM) but suffered from potent CYP450 inhibition (3A4, IC$_{50}$ < 1 μM), a common problem among the propargyl analogues. Replacement of the propargyl unit with a simple

Table 1. Enzymatic and Cellular Activities of Select 2-Aminopyridine Analogues[a]

Compd	R[1]	R[2]	IC$_{50}$ (nM) Met[b]	IC$_{50}$ (nM) GTL-16 IC[c]
3	(4-methylpiperazinyl ethyl)	H	5.9±0.8	2800
4	H$_2$N-propargyl	H	3.8±1.5	210
5	HO-propargyl	H	2.7±0.6	23
6	HO-ethyl	H	3.4±0.5	280
7	propargyl	H	1.0±0.2	31
8	CH(CH$_3$)$_2$	H	3.4±1.5	120
9	Cl	H	1.0±0.1	57
10	Cl	OEt	3.9±0.5	100
11	Cl	OCH(CH$_3$)$_2$	3.2±1.0	140
12	Cl	OCH$_2$CH$_2$OH	2.6±0.3	250

[a] See ref 6 for a description of assay conditions. [b] IC$_{50}$ values are reported as the mean of at least three independent determinations. [c] Met-dependent human gastric carcinoma cell line.

branched alkyl group such as isopropyl provided no benefit (**8**, IC$_{50}$ = 3.4 nM, GTL-16 IC$_{50}$ = 120 nM). Finally, 3-chloro analogue **9** was found to potently inhibit Met kinase with an IC$_{50}$ of 1.0 nM while maintaining excellent cellular potency (GTL-16 IC$_{50}$ = 57 nM). Chloro-substituted aminopyridine **9** benefited from excellent stability in mouse liver microsomes (MLM = 0.012 (nmol/min)/mg protein) and an encouraging CYP450 profile (3A4 IC$_{50}$ = 4 μM; 2C9 IC$_{50}$ = 7 μM; 2C19, 2D6, 1A2 IC$_{50}$ values of >20 μM); therefore, it was selected as a scaffold for pyridone SAR exploration to improve kinase selectivity and the CYP450 profile.

A series of alkoxy groups was appended to the pyridone ring at R^2 (Table 1). Ethoxy analogue **10** inhibited Met kinase with an IC$_{50}$ of 3.9 nM (GTL-16 IC$_{50}$ = 100 nM). In addition, compound **10** demonstrated >40-fold improvement in aqueous solubility at pH 1.0 (aqueous solubility = 400 μg/mL, crystalline).[7] The dramatic improvement in aqueous solubility can be attributed to a deviation from planarity induced by the R^2 substituent which results in disruption of crystal packing forces (vide infra). Replacement of the R^1 chlorine atom of **10** with other halogens (e.g., F, Br) or a methyl substituent provided analogues with inferior cellular potency. Additional alkoxy groups were examined at R^2 with isopropoxy analogue **11** giving an in vitro potency (IC$_{50}$ = 3.2 nM, GTL-16 IC$_{50}$ = 140 nM) similar to that of **10**. Likewise, introduction of an alcohol provided no benefit (**12**, IC$_{50}$ = 2.6 nM, GTL-16 IC$_{50}$ = 250 nM). On the basis of its relatively low molecular weight,

Scheme 1[a]
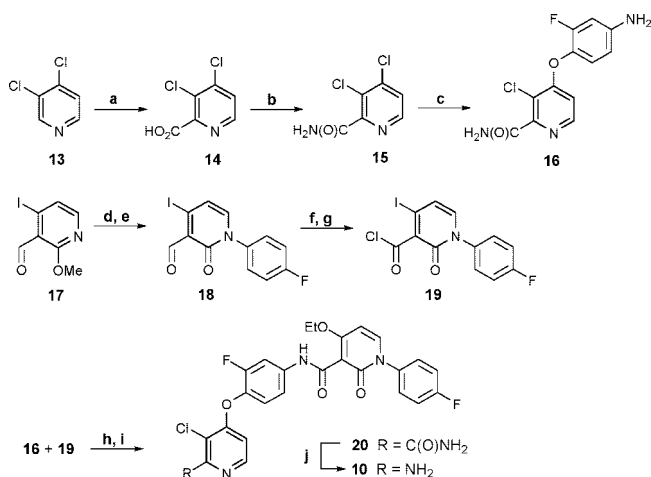
[a] Reagents and conditions: (a) LiTMP, ether, −78 °C, then CO$_2$, 39%; (b) SOCl$_2$, 80 °C, then NH$_4$OH, 0 °C, 76%; (c) 4-amino-2-fluorophenol, KO-*t*-Bu, DMF, 50 °C, 79%; (d) TMSI, CH$_3$CN, 90%; (e) 4-fluorophenylboronic acid, Cu(OAc)$_2$, 2,6-lutidine, myristic acid, toluene, 68%; (f) NaOCl, 2-methyl-2-butene, NaH$_2$PO$_4$, THF/*t*-BuOH/H$_2$O, 70%; (g) SOCl$_2$, toluene; (h) DIPEA, THF/DMF, 89% (two steps); (i) NaOEt, EtOH, THF, 95%; (j) PhI(OAc)$_2$, EtOAc/CH$_3$CN/H$_2$O, 74%.

improved aqueous solubility, attractive in vitro profile, and desirable metabolic stability/CYP450 profile (IC$_{50}$ values > 20 μM), **10** was selected for further characterization in kinase selectivity, PK, and in vivo efficacy studies.

Compound **10** was prepared according to the synthetic sequence outlined in Scheme 1. Commercially available 3,4-dichloropyridine **13** was converted to acid **14** by deprotonation with LiTMP and quenching with dry ice.[8] The resulting acid was converted to amide **15** under standard conditions. Nucleophilic displacement of the C-4 chloride of **15** with 4-amino-2-fluorophenol gave key intermediate **16**. The pyridone subunit **19** was synthesized from 4-iodo-2-methoxynicotinaldehyde.[9] Thus, the methyl ether of **17** was cleaved with TMSI and the resulting amide was arylated with 4-fluorophenylboronic acid using copper(II) acetate.[10] Oxidation of aldehyde **18** to the corresponding acid followed by acid chloride formation gave intermediate **19**. Amine **16** and acid chloride **19** were joined under standard conditions, and the iodide was reacted with sodium ethoxide to give ethyl ether **20**. Finally, Hoffman rearrangement delivered **10** in high yield.

An X-ray crystal structure of **10** complexed to the Met kinase domain confirmed that **10** resides in the ATP-binding site with the activation loop in an inactive, DFG-out conformation (Figure 1).[11] The 2-aminopyridine core anchors inhibitor **10** to the hinge region via two key hydrogen bonding interactions with Met1160; the backbone NH of Met1160 donates a hydrogen bond to the pyridine nitrogen, while the backbone carbonyl of Met1160 accepts a hydrogen bond from the 2-amino group. As postulated, the 3-chloro group is directed toward the ribose pocket. The central phenyl ring π-stacks with Phe1223 (DFG motif) and is flanked on the opposite face by gatekeeper residue Leu1157. The pyridone carbonyl forms an intramolecular hydrogen bond with the amide NH and a second hydrogen bond with the backbone NH of Asp1222. Finally, the terminal phenyl ring occupies a deep hydrophobic pocket defined by Phe1134, Leu1195, and Phe1200.

Compound **10** was evaluated in an in-house kinase selectivity panel (Table 2). The K_i was determined for Met kinase (K_i = 4.6 ± 0.3 nM), and while **10** was found to be a potent inhibitor of Met family member Ron and three phylogenetically related
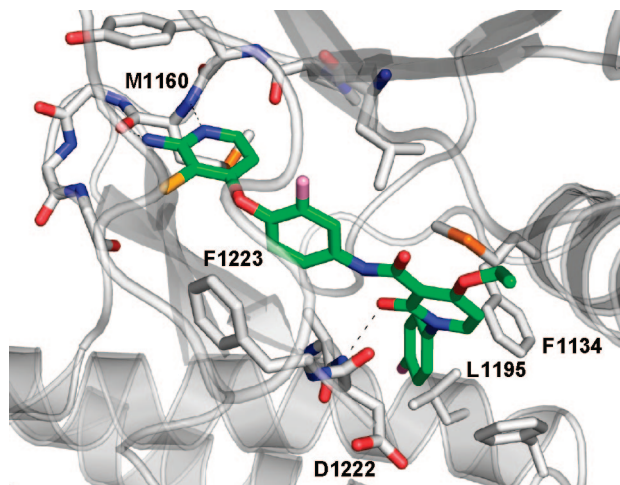
Figure 1. X-ray crystal structure of **10** bound to the Met kinase domain (1067−1378, triple mutant Y1212F, Y1252F, Y1253D).[11]

Table 2. Kinase Selectivity Profile of **10**

kinase	enzyme IC$_{50}$, nM	kinase	enzyme IC$_{50}$, nM
Met	3.9	BTK	>2000
Axl	1.1	CDK2E	>2000
Ron	1.8	EGFR	>2000
Tyro3	4.3	GSK-3β	>2000
Mer	14	IGFR-1R	>2000
Flt-3	16	IKK1/2	>2000
AurB	78	InsR	>2000
Lck	120	Jak2	>2000
VEGFR-2	180	MK2	>2000
TrkB	190	P38α	>2000
TrkA	290	Pim-1	>2000
PKA	550	Plk-1/3	>2000

kinases (Axl, Tyro-3, and Mer), it was more than 40-fold selective versus Lck, VEGFR-2, and TrkA/B and more than 500-fold selective versus all other receptor and nonreceptor kinases in the panel. To further examine its selectivity, **10** was profiled against more than 200 kinases in the Ambit phage-based competition binding assay (Figure 2).[12] In this assay, results are reported as % control at a 10 μM screening
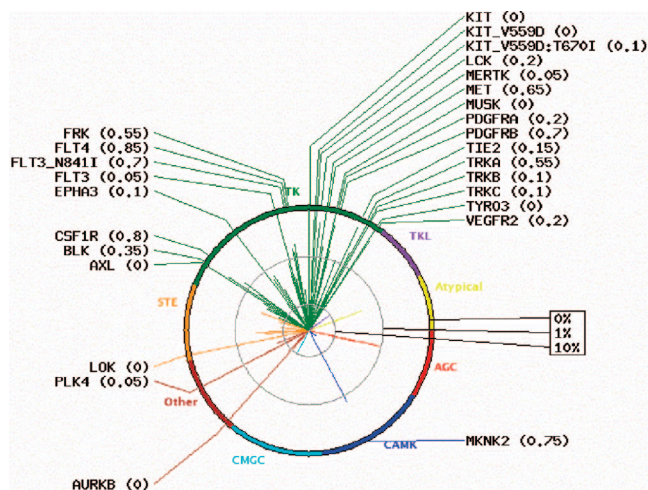

Figure 2. Radial plot of Ambit competition binding assay. The logit transformation was applied [logit = $x/(100 - x)$]. Abbreviations: TK, tyrosine kinase; TKL, tyrosine kinase-like; AGC, protein kinase A, G, and C families; CAMK, calcium-calmodulin dependent kinases; CMGC, cyclin dependent kinases, mitogen-activated protein kinases, glycogen synthase kinase-3, cyclin dependent kinase-like; STE, homologues of yeast sterile 7, 11, 20 kinases.
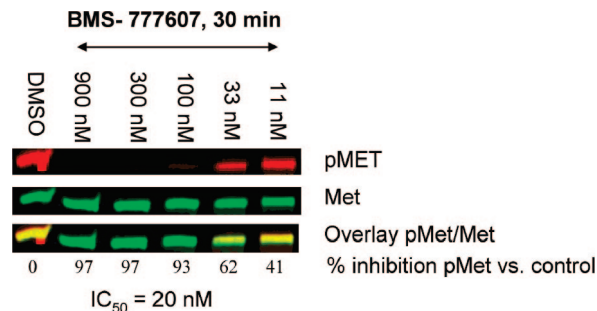

Figure 3. Phospho Met protein levels in GTL-16 cell lysates.

Table 3. Pharmacokinetic Parameters for **10** in Mouse, Rat, and Dog[a]

parameter	mouse[b]	rat[c]	dog
po dose (mg/kg)	10	10	5[c]
iv dose (mg/kg)	5	5	1[d]
C_{max} (μM), po	17.6	8.7 ± 4.2	29.0 ± 6.9
T_{max} (h), po	0.5	1.7 ± 0.6	2.3 ± 1.5
AUC$_{0-24h}$ (μM·h), po	90	37.7 ± 19.2	198 ± 68
$t_{1/2}$ (h), iv	4.5	4.8 ± 1.5	4.9
Cl (mL min^{-1} kg^{-1}), iv	4.4	12.1 ± 1.4	0.82
V_{ss} (L kg^{-1}), iv	1.2	1.0 ± 0.1	0.22
F_{po} (%)	100	100	100

[a] Vehicle: 70% PEG400−30% water. [b] Data reported as an average of six animals. [c] Data reported as an average of three animals. [d] Data reported as an average of two animals.

concentration. A result of <1% control correlates with a K_d < 1−3 μM. As expected, Met-related kinases (Ron, Axl, Tyro-3, Mer) and several other kinases from Table 2 (AurB, Flt-3, Lck, TrkA/B) registered binding of <1% control. A handful of other kinases registered <1% control and were followed up in a two-point assay where IC$_{50}$ values were estimated to be between 50 and 500 nM (LOK, Tie-2, Mnk2, Musk) or >500 nM (Blk, Epha3, Kit, Src). A cellular proliferation assay was used to determine the IC$_{50}$ for PDGFRβ (IC$_{50}$ = 1 μM). To conclude, our in-house kinase selectivity panel and the Ambit binding assay confirmed **10** to be a potent and selective inhibitor of the Met kinase superfamily.

The antiproliferative activity of **10** was explored in additional cellular settings, and **10** demonstrated selective inhibition of proliferation in Met-driven tumor cell lines. In addition to potent inhibition of proliferation of the GTL-16 cell line, which contains an amplified Met gene locus, **10** also inhibited proliferation in Met-driven H1993 (non-small-cell lung cancer, Met amplification, IC$_{50}$ = 150 nM) and U87 (glioblastoma, autocrine loop, IC$_{50}$ = 160 nM) cell lines. Importantly, **10** lacked activity against the Met-independent N87 cell line (gastric, IC$_{50}$ > 10 000 nM).

Phosphorylation levels of the Met protein in GTL-16 cell lysates was determined following a 30 min incubation period (Figure 3). Phosphorylation of the Met receptor was inhibited in a concentration-dependent manner, consistent with the observed in vitro activity and also consistent with the activity in GTL-16 cells being a result of Met kinase inhibition.

The pharmacokinetic parameters obtained for **10** in mouse, rat, and dog are summarized in Table 3. After iv administration, **10** demonstrated a moderate steady-state volume of distribution (V_{ss}) in mouse and rat and low systemic clearance (Cl) compared to hepatic blood flow for all species. The compound was well absorbed after oral administration of drug from solution formulation with favorable half-lives ($t_{1/2}$) and mean residence times (MRT). Furthermore, the measured oral bioavailabilities (F_{po}) were excellent in all three species (100%).[13]
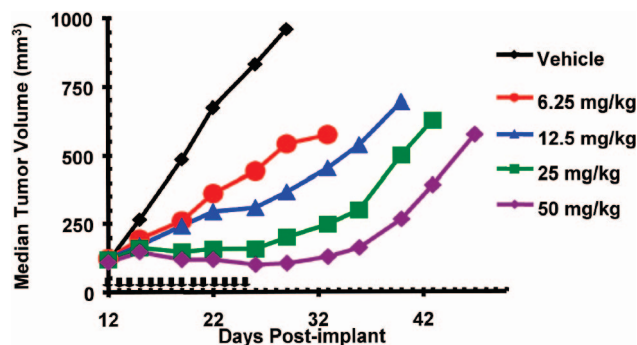
Figure 4. In vivo efficacy of **10** versus GTL-16 human tumor xenografts in athymic mice (1qd x 14).

On the basis of its encouraging pharmacokinetic profile, **10** was evaluated in in vivo efficacy studies (Figure 4). A GTL-16 xenograft model was examined in which tumor cells were implanted subcutaneously and staged to approximately 125 mm^3 prior to commencement of once daily oral dosing of compound for 14 consecutive days. Compound **10** was active at all dose levels tested as defined by >50% tumor growth inhibition (TGI) over one tumor volume doubling time (TVDT).[14] The minimum efficacious dose of 6.25 mg/kg corresponded to a TGI of 66%, and complete tumor stasis was observed throughout the dosing period at 25 and 50 mg/kg doses (TGI = 95% and 102%, respectively). The antitumor activity of **10** was dose responsive, and the measured drug exposures at each dose level were dose proportional (6.25 mg/kg, C_{max} = 4.5 μM, AUC_{0-24h} = 37 μM·h; 50 mg/kg, C_{max} = 43.7 μM, AUC_{0-24h} = 567 μM·h). No overt toxicity was observed at any of these dose levels as defined by weight loss or morbidity.

In conclusion, novel substituted N-(4-(2-aminopyridin-4-yloxy)-3-fluoro-phenyl)-1-(4-fluorophenyl)-2-oxo-1,2-dihydro-pyridine-3-carboxamides were identified as potent inhibitors of Met kinase activity. Optimization of the series SAR led to identification of **10**, a highly selective and orally bioavailable Met kinase inhibitor. Complete tumor stasis was achieved in the GTL-16 human gastric carcinoma xenograft model following oral administration with no observed toxicity. On the basis of its favorable in vivo efficacy, pharmacokinetic profile, and safety profile, **10** has been advanced into clinical trials.

Supporting Information Available: Characterization data for **2−12**, experimental procedures for **10**, and detailed description of pharmacokinetic assays. This material is available free of charge via the Internet at http://pubs.acs.org.

References

(1) Recent reviews on Met kinase: (a) Liu, X.; Yao, W.; Newton, R. C.; Scherle, P. A. Targeting the c-Met signaling pathway for cancer. *Expert. Opin. Invest. Drugs* **2008**, *17*, 997–1011. (b) Peruzzi, B.; Bottaro, D. P. Targeting the c-Met signaling pathway in cancer. *Clin. Cancer Res.* **2006**, *12*, 3657–3660. (c) Christensen, J. G.; Burrows, J.; Salgia, R. c-Met as a target for human cancer and characterization of inhibitors for therapeutic intervention. *Cancer Lett.* **2005**, *225*, 1–26.

(2) Jarvis, L. M. Targeting the c-Met signaling pathway for cancer therapy. *Chem. Eng. News* **2007**, *85*, 15–23.

(3) (a) Stewart, F. Roles of mesenchymal−epithelial interactions and hepatocyte growth factor−scatter factor (HGF-SF) in placental development. *Rev. Reprod.* **1996**, *1*, 144–148. (b) Huh, C.-G.; Factor, V. M.; Sanchez, A.; Uchida, K.; Conner, E. A.; Thorgeirsson, S. S. Hepatocyte growth factor/c-met signaling pathway is required for efficient liver regeneration and repair. *Proc. Natl. Acad. Sci. U.S.A.* **2004**, *101*, 4477–4482.

(4) Schroeder, G. M.; Chen, X.-T.; Williams, D. K.; Nirschl, D. S.; Cai, Z.-W.; Wei, D.; Tokarski, J. S.; An, Y.; Sack, J.; Chen, Z.; Huynh, T.; Vaccaro, W.; Poss, M.; Wautlet, B.; Gullo-Brown, J.; Kellar, K.; Manne, V.; Hunt, J. T.; Wong, T. W.; Lombardo, L. J.; Fargnoli, J.; Borzilleri, R. M. Identification of pyrrolo[2,1-*f*][1,2,4]triazine-based inhibitors of Met kinase. *Bioorg. Med. Chem. Lett.* **2008**, *18*, 1945–1951.

(5) Cai, Z.-W.; Wei, D.; Schroeder, G. M.; Cornelius, L. A. M.; Kim, K.; Chen, X.-T.; Schmidt, R. J.; Williams, D. K.; Tokarski, J. S.; An, Y.; Sack, J. S.; Manne, V.; Kamath, A.; Zhang, Y.; D'Arienzo, C.; Marathe, P.; Hunt, J. T.; Trainor, G. L.; Lombardo, L. J.; Fargnoli, J.; Borzilleri, R. M. Discovery of orally active pyrrolopyridine- and aminopyridine-based Met kinase inhibitors. *Bioorg. Med. Chem. Lett.* **2008**, *18*, 3224–3229.

(6) Kim, K. S.; Zhang, L.; Schmidt, R.; Cai, Z.-W.; Wei, D.; Williams, D. K.; Lombardo, L. J.; Trainor, G. L.; Xie, D.; Zhang, Y.; An, Y.; Sack, J. S.; Tokarski, J. S.; D'Arienzo, C.; Kamath, A.; Marathe, P.; Zhang, Y.; Lippy, J.; Jeyaseelan, R.; Wautlet, B.; Henley, B.; Gullo-Brown, J.; Manne, V.; Hunt, J. T.; Fargnoli, J.; Borzilleri, R. M. Discovery of pyrrolopyridine-pyridone based inhibitors: synthesis, X-ray crystallographic analysis, and biological activities. *J. Med. Chem.* **2008**, *51*, 5330–5341.

(7) Aqueous solubility at pH 6.5 is 2 μg/mL (crystalline).

(8) Marzi, E.; Bigi, A.; Schlosser, M. Strategies for the selective functionalization of dichloropyridines at various sites. *Eur. J. Org. Chem.* **2001**, *7*, 1371–1376.

(9) Fang, F. G.; Xie, S.; Lowery, M. W. Catalytic enantioselective synthesis of 20(2)-camptothecin: a practical application of the Sharpless asymmetric dihydroxylation reaction. *J. Org. Chem.* **1994**, *59*, 6142–6143.

(10) Antilla, J. C.; Buchwald, S. L. Copper-catalyzed coupling of arylboronic acids and amines. *Org. Lett.* **2001**, *3*, 2077–2079.

(11) The structure was deposited in the PDB as 3F82.

(12) Fabian, M. A.; Biggs, W. H., III; Treiber, D. K.; Atteridge, C. R.; Azimioara, M. D.; Benedetti, M. G.; Carter, T. A.; Ciceri, P.; Edeen, P. T.; Floyd, M.; Ford, J. M.; Galvin, M.; Gerlach, J. L.; Grotzfeld, R. M.; Herrgard, S.; Insko, D. E.; Insko, M. A.; Lai, A. G.; Lelias, J.-M.; Mehta, S. A.; Milanov, Z. V.; Velasco, A. M.; Wodicka, L. M.; Patel, H. K.; Zarrinkar, P. P.; Lockhart, D. J. A small molecule−kinase interaction map for clinical kinase inhibitors. *Nat. Biotechnol.* **2005**, *23*, 329–336.

(13) Protein binding was >99% across species.

(14) TGI = {$(C_t - T_t)/(C_t - C_0)$} × 100, where C_t = the median tumor volume (mm^3) of vehicle-treated control mice at time t, T_t = median tumor volume of treated mice at time t, and C_0 is the median tumor volume of control mice at time 0.